The Influence of Rifabutin on Human and Bacterial Membrane Models: Implications for Its Mechanism of Action

ARTICLE *in* THE JOURNAL OF PHYSICAL CHEMISTRY B · APRIL 2013

Impact Factor: 3.3 · DOI: 10.1021/jp403073v · Source: PubMed

7 AUTHORS, INCLUDING:

João Miguel Caio
University of Aveiro
13 PUBLICATIONS **70** CITATIONS
SEE PROFILE

Cristina Moiteiro
University of Lisbon
32 PUBLICATIONS **239** CITATIONS
SEE PROFILE

Marlene Lúcio
University of Minho
60 PUBLICATIONS **889** CITATIONS
SEE PROFILE

THE JOURNAL OF PHYSICAL CHEMISTRY B

Article

pubs.acs.org/JPCB

The Influence of Rifabutin on Human and Bacterial Membrane Models: Implications for Its Mechanism of Action

Marina Pinheiro,[†] Cláudia Nunes,[†] João M. Caio,[‡] Cristina Moiteiro,[‡] Marlene Lúcio,[†] Gerald Brezesinski,[§] and Salette Reis*[,†]

[†]REQUIMTE, Departamento de Ciências Químicas, Faculdade de Farmácia, Universidade do Porto, Portugal

[‡]Centro de Química e Bioquímica, Departamento de Química e Bioquímica, Faculdade de Ciências, Universidade de Lisboa, Portugal

[§]Department of Interfaces, Max Planck Institute of Colloids and Interfaces, Science Park Golm, 14476 Potsdam, Germany

ABSTRACT: This work focuses on the interaction of the antibiotic Rifabutin (RFB) with phospholipid membrane models using small- and wide-angle X-ray scattering (SAXS and WAXS) to assess drug–membrane interactions. The effect of different concentrations of RFB on human and bacterial cell membrane models was studied using multilamellar vesicles (MLVs) at the physiological pH (7.4). In this context, MLVs of 1,2-dimyristoyl-*rac*-glycero-3-phosphocholine (DMPC) were chosen to mimic the human cell membrane. To mimic the bacterial cell membrane, 1,2-dimyristoyl-*sn*-glycero-3-phospho-*rac*-(1-glycerol) (DMPG) and a mixture of 1,2-dipalmitoyl-*sn*-glycero-3-phosphoethanolamine (DPPE) and 1,2-dipalmitoyl-*sn*-glycero-3-phospho-*rac*-(1-glycerol) (DPPG) (8:2 molar ratio) were used. The results support a perturbation of the lipid bilayers caused by RFB, especially in the bacterial membrane model, inducing phase separation that might compromise the integrity of the bacterial membrane. Therefore, the different effects of this antibiotic depending on the concentration, the charge of the phospholipid headgroup, and the membrane organization may be related with the RFB antibiotic activity and the side effects, and should be accounted for during the anti-tuberculosis (anti-TB) drug design.

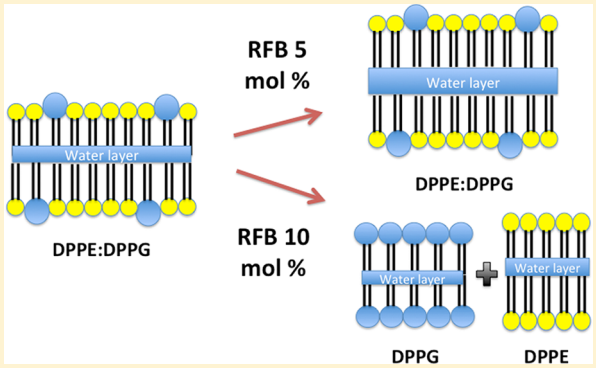

1. INTRODUCTION

Rifabutin (RFB, Figure 1) is a wide spectrum antibiotic used in the treatment of mycobacterial infectious diseases.[1] It is used as a second-line anti-tuberculosis (anti-TB) drug regarding its high activity against *Mycobacterium tuberculosis* (MTB), the etiological agent of tuberculosis (TB). This semisynthetic derivate of ryfamicin is less prone to the interactions with the antiretroviral drugs than the first-line-drug rifampicin (also a derivate of ryfamicin), being therefore mostly used as the first choice in the HIV (human immunodeficiency virus)-TB coinfected patients.[2] RFB has an intracellular target, namely, the enzyme RNA polymerase, and therefore, it must pass across the human and mycobacterial membranes to reach the pharmacological target. Nevertheless, a lack of correlation exists between the inhibitory activity of ryfamicins on the RNA polymerase and the antibiotic efficacy, with the efficacy mainly being attributed to the drug's penetration into the cells.[3] In fact, it is well-known that part of the success of RFB as an antimycobacterial compound is related with its high membrane lipid tropism and high penetration into the infected cells such as the alveolar macrophages in the lungs. For instance, RFB accumulates in the lungs at levels 6 times higher when compared with the plasma concentrations. The high lipid affinity of RFB seems to be responsible for the discrepancy between the plasma concentrations and the much higher concentrations achieved in the tissues and infected cells.[2] Additionally, our previous work contributes to the elucidation of the higher drug accumulation in the lungs due to a distribution at the pulmonary surfactant lipid level, evidenced by the inclusion complex formed between the drug and the polar head groups of the phospholipids. On the other hand, the inclusion complex formed by the drug is restricted to the polar head groups of the phospholipids, which might explain the low toxicity to the lungs despite the high drug concentrations reaching this organ.[3] In addition, the side effects of RFB, such as uveitis and discoloration of the skin, seem to be related to its affinity and ability to cross the biological membranes.[3]

To mimic the cell membranes, multilamellar vesicles (MLVs) were used as reliable cell membrane models, which allow one to study the drug–membrane interactions, since they account for the most relevant process of the drug's permeation across the bilayers (i.e., the diffusion).[3] The phosphatidylcholines represent the major components of the outer layer of the human membranes and are practically absent in bacterial membranes.[4] Hence, DMPC (Figure 1), a zwitterionic phospholipid, was chosen as a simple but suitable membrane model of the human cell membrane for mimicking the neutral charge of the surface membrane of eukaryotic plasma membranes.[4] On the other side, DMPG (Figure 1), a negatively

Received: March 28, 2013
Published: April 25, 2013

   dx.doi.org/10.1021/jp403073v | *J. Phys. Chem. B* 2013, 117, 6187–6193

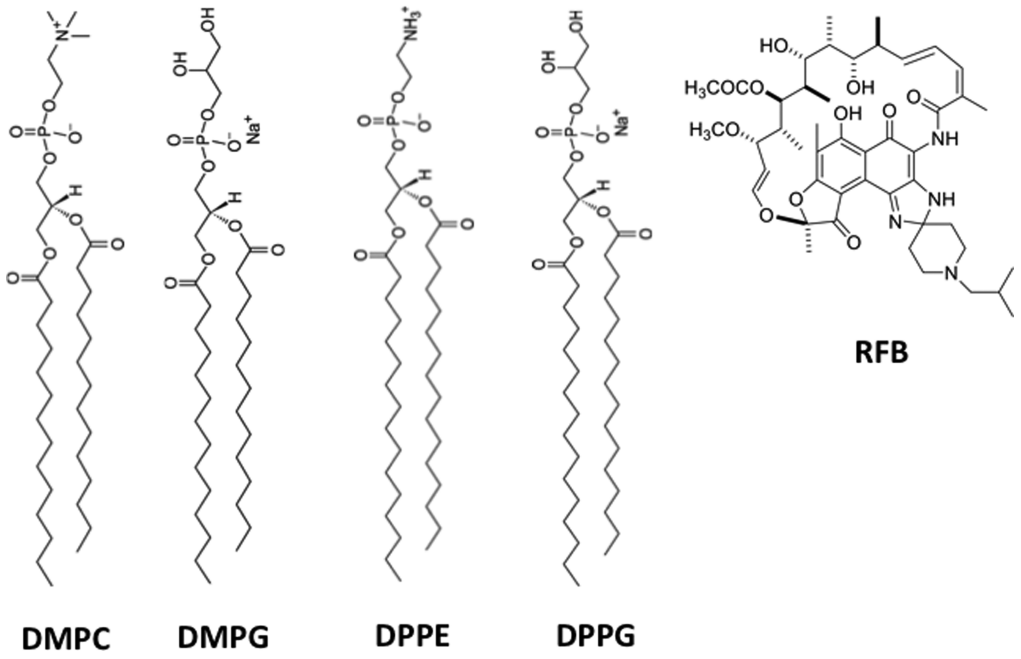

Figure 1. Chemical structure of 1,2-dimyristoyl-*rac*-glycero-3-phosphocholine (DMPC), 1,2-dimyristoyl-*sn*-glycero-3-phospho-*rac*-(1-glycerol) (DMPG), 1,2-dipalmitoyl-*sn*-glycero-3-phospho-*rac*-(1-glycerol), 1,2-dipalmitoyl-*sn*-glycero-3-phosphoethanolamine (DPPE), and rifabutin (RFB).

charged lipid, was chosen as the bacterial cell membrane model, mimicking the negative charge of the inner plasma membrane.[3] In addition, DPPE:DPPG (Figure 1) 8:2 (molar ratio) was the selected composition of a more complex bacterial membrane model, with the phosphatidylethanolamines also being one of the major constituents of the bacterial membranes.[5,6]

Small-angle X-ray scattering (SAXS) and wide-angle X-ray scattering (WAXS), two powerful X-ray techniques, were used in this study to assess the drug−membrane model interaction.

The experimental results point to a more pronounced interaction of RFB with the bacterial membrane models, which is ascribed for the electrostatic interactions between RFB and the polar head groups of the phospholipids, which may promote the disturbance of the bacterial membrane and consequently the bacterial cell death.

2. MATERIALS AND METHODS

2.1. Materials. DMPC and DMPG were purchased from Sigma-Aldrich Co. DPPG and DPPE were purchased from Avanti Polar Lipids. RFB was isolated from Mycobutin and further purified as previously described.[2] *N*-(2-Hydroxyethyethyl)piperazine-*N*′-(2-ethanesulfonic acid) (HEPES) and sodium chloride (NaCl) were purchased from Sigma-Aldrich Co. The buffer system (HEPES 0.01 M, pH 7.4, I = 0.1 M) was prepared with ultrapure water produced by Millipore Milli-Q (resistivity = 18.2 MΩ cm), and the ionic strength was adjusted with NaCl.

2.2. Methods. *2.2.1. Mutilamellar Vesicles.* Different amounts of RFB were mixed with DMPC, DMPG, and DPPE:DPPG (8:2 molar ratio) in a chloroform:methanol mixture (3:1 v/v) according to the required molar fraction of the drug (5 and 10 mol %). Lipid films were formed from these solutions, dried at 65.0 ± 0.1 °C under a stream of N_2, and left overnight under reduced pressure to remove all traces of the organic solvents. The lipid films were hydrated by adding the buffer system and then alternately heated to 65.0 ± 0.1 °C, mixed by vortexing for about 5 min, and centrifuged for 30 s at 2000*g*. This procedure was repeated three times. Finally, the samples were aged overnight at 4.0 ± 0.1 °C and shaken by vortex at room temperature for 5 min. Thereafter, the dispersions were transferred into glass capillaries of 1.5 mm diameter (Hilgenberg, Malsfeld, Germany), which are transparent to X-rays. The flame-sealed capillaries were stored at 4.0 ± 0.1 °C until the measurements.

2.2.2. Small Angle X-ray Scattering and Wide Angle X-ray Scattering. SAXS and WAXS experiments were executed at beamline A2 at Doris III of HASYLAB (DESY, Hamburg, Germany) using monochromatic radiation with a wavelength of 0.15 nm. The SAXS detector was calibrated with rat-tail tendon and the WAXS detector with polyethyleneterephthalat (PET). Heating scans from 8 to 70 °C were performed at a rate of 1 K min^{-1}. Data was recorded for 10 s every minute. The samples were also exposed to static measurements according to the thermotropic behavior of the lipids. After each temperature step, the sample was allowed to equilibrate for 5 min before the diffraction pattern was recorded. In order to minimize the X-ray exposure to the sample, a shutter mounted before the sample was kept closed when no data was acquired. The lamellar repeat distance d was calculated from the diffraction patterns using Bragg's equation $s = n/d$, where $s = (2 \sin \Theta)/\lambda$ is the scattering vector and n the order of the reflection (n = 1, 2, ...). To obtain the precise position of the Bragg peaks, Lorentzian curves were fitted to the diffraction peaks, and the positions of maximum intensities as well as the full width at half-maximum (fwhm) were determined.[4]

3. RESULTS AND DISCUSSION

The interaction of RFB with DMPC, DMPG, and DPPE:DPPG was investigated using X-ray diffraction patterns at small and wide angles, yielding information, respectively, on long-range bilayer organization and hydrocarbon chain packing.[7] The SAXS and WAXS studies were carried out in a range of temperature from 8 to 70 °C, with the purpose of elucidating the different lipid phases and assessing the

dx.doi.org/10.1021/jp403073v | J. Phys. Chem. B 2013, 117, 6187−6193

Table 1. Long Distances (d) of DMPC Bilayers and Correlation Lengths (ξ) Determined from SAXS Diffraction Patterns at pH 7.4 and at 10, 18, and 40 °C[a]

		d_{SAXS} (Å)			
sample (mol % RFB)	T (°C)	d_1	d_2	ξ_1 (Å)	ξ_2 (Å)
DMPC:RFB 0	10	61.2 ± 0.5		678 ± 10	
	18	66.8 ± 0.5		604 ± 10	
	40	62.6 ± 0.5		629 ± 10	
DMPC:RFB 5	10	62.4 ± 0.5		968 ± 10	
	18	71.9 ± 0.5		789 ± 10	
	40	63.4 ± 0.5		590 ± 10	
DMPC:RFB 10	10	64.4 ± 0.5		825 ± 10	
	18	70.7 ± 0.5		866 ± 10	
	40	64.7 ± 0.5	61.7 ± 0.5	498 ± 10	797 ± 10

[a]The data are presented in Å as a function of the 5 and 10 mol % RFB.

transition temperatures between these phases. Additionally, static measurements were also performed, according to the thermotropic behavior of the lipids to the Lβ', Pβ', and Lα phases and specifically at 10, 18, and 40 °C for DMPC and 8, 18, and 40 °C for DMPG, respectively. For the lipid mixture DPPE:DPPG, the investigated temperatures were 37, 56, and 65 °C in order to study the structures of the gel and fluid phases. In the presence of excess water, the mentioned lipids form lyotropic lamellar phases whose structure and organization are dependent on the temperature. DMPC and DMPG form three different phases, namely, Lβ', Pβ', and Lα, depending on the temperature. The lipid mixture DPPE:DPPG (8:2 molar ratio) seems to have only two different phases (Lβ' and Lα). The Lβ' corresponds to the gel phase in which the acyl chains are in an all-*trans* conformation and tilted. The temperature increase leads to the pretransition from Lβ' to Pβ' (in the case of DMPC and DMPG), in which the lipid bilayers are distorted by a periodic ripple in the lamellae plane. Further temperature increase leads to the main lipid phase transition to the liquid-crystalline Lα phase: in the case of DMPC and DMPG (Pβ' → Lα) or in the case of the lipid mixture DPPE:DPPG (Lβ' → Lα). In the liquid-crystalline Lα phase, the acyl chains are disordered (*trans*–*gauche* isomerization).[8]

3.1. Effects of RFB on the Structure of DMPC Bilayers.

The repeat distances d deduced from the SAXS patterns of DMPC in the absence and presence of RFB are depicted in Table 1. For DMPC, the Bragg peaks appear at 1/61.2 Å^{-1} (Lβ'), 1/66.8 Å^{-1} (Pβ'), and 1/62.6 Å^{-1} (Lα), and are in close agreement with the literature data.[9] In addition, the repeat distances d, deduced from the WAXS patterns of DMPC in the absence and in the presence of RFB, are represented in Table 2. Analyzing Table 2, the diffraction pattern of DMPC at 10 °C displays a sharp reflection at 1/4.13 Å^{-1} with a shoulder located at 1/3.96 Å^{-1}, which reflects the orthorhombic (pseudohexagonal) lattice of the chains in the bilayers, characteristic of the Lβ' phase.[10] At 18 °C, only one diffraction peak is observed at 1/4.15 Å^{-1} with a symmetric profile, indicating a hexagonal chain packing characteristic of the Pβ' phase.[10,11] At 40 °C, in the Lα phase, a broad halo appears, which corresponds to the disordered molten chains (data not shown).[9] Furthermore, the main transition occurs at 22–24 °C, connected with the disappearance of the well-defined WAXS peaks (data not shown).[12]

Table 2. Short Distances (d) of DMPC Bilayers and Correlation Lengths (ξ) Determined from WAXS Diffraction Patterns at pH 7.4 and at 10, 18, and 40 °C[a]

		d_{WAXS} (Å)			
sample (mol % RFB)	T (°C)			ξ_1 (Å)	ξ_2 (Å)
DMPC 0	10	4.13	3.96	49 ± 10	82 ± 10
	18	4.15		80 ± 10	
DMPC:RFB 5	10	4.13		40 ± 10	
	18	4.18		30 ± 10	
DMPC:RFB 10	10	4.14		41 ± 10	
	18	4.19		31 ± 10	

[a]The data are presented in Å as a function of the 5 and 10 mol % RFB.

The incorporation of RFB into the DMPC MLVs is responsible for pronounced changes in the SAXS patterns with a d-spacing increase in the gel phases (Table 1). Therefore, in both gel phases (Lβ' and Pβ'), the bilayer thickness, including the water layer between the bilayers, increases up to approximately 5 Å. Moreover, this effect seems to be dependent on the drug concentration in the Lβ' phase. In the Lα phase, considered to be the most biologically relevant mesophase, 5 mol % RFB does not change the d-spacing (within the experimental error) (Figure 2). However, two lamellar phases with different d-spacings are observed in samples with 10 mol % RFB (Figure 2). Therefore, a noninfluenced DMPC phase (since the d values are not relevantly changed in comparison with pure DMPC) and a mixed DMPC phase with a higher d value coexist. The correlation length between the bilayers (ξ) increases in the gel phase due to the incorporation of RFB, whereas in the fluid phase a decrease of the correlation length is observed.

The evaluation of the WAXS pattern in the gel phases (Lβ' and Pβ') (Table 2) confirms that RFB changes the lattice constants and the correlation length ξ in a non-concentration-dependent manner, which is consistent with the pronounced interactions with the phospholipid head groups and with the membrane disordering effect in the most organized and tightly packed phospholipid phases. The WAXS diffraction pattern of DMPC in the absence and in the presence of 10 mol % RFB at 10 °C is shown in Figure 3. The WAXS spectrum of DMPC in the presence of 10 mol % RFB displays a single, symmetrical but quite broad peak, which points to a hexagonal hydrocarbon chain packing induced by RFB (Figure 3).[10]

Furthermore, RFB is a bulky and amphiphilic molecule, which contains some groups that can be protonated (piperidine nitrogen and imidazole nitrogen) and deprotonated (naphthol oxygen) depending on the pH value. At a pH of 7.4, while the zwitterionic species predominate (83.4%), a significant contribution of positively charged molecules (roughly 16.6%) (predicted using MarvinView 5.4.1.1 software from ChemAx-

dx.doi.org/10.1021/jp403073v | J. Phys. Chem. B 2013, 117, 6187–6193

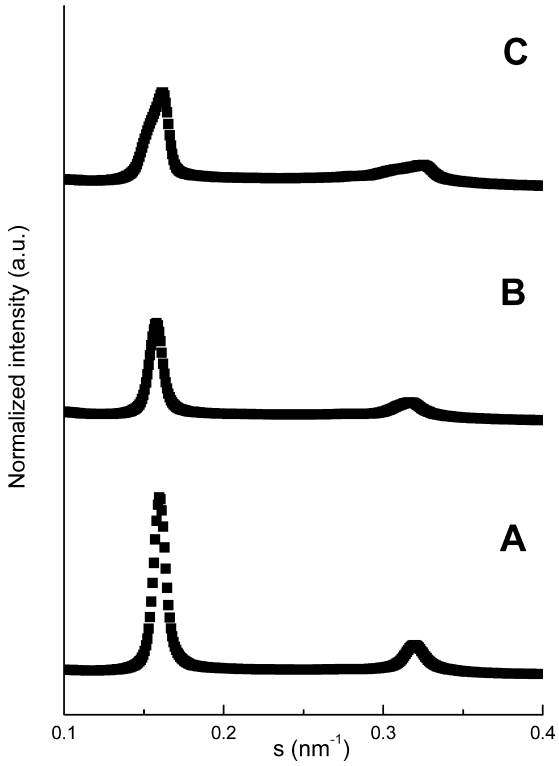

Figure 2. Small-angle X-ray diffraction profiles of DMPC (A) and mixtures of DMPC with RFB at 5 mol % (B) and 10 mol % (C) at 40 °C.

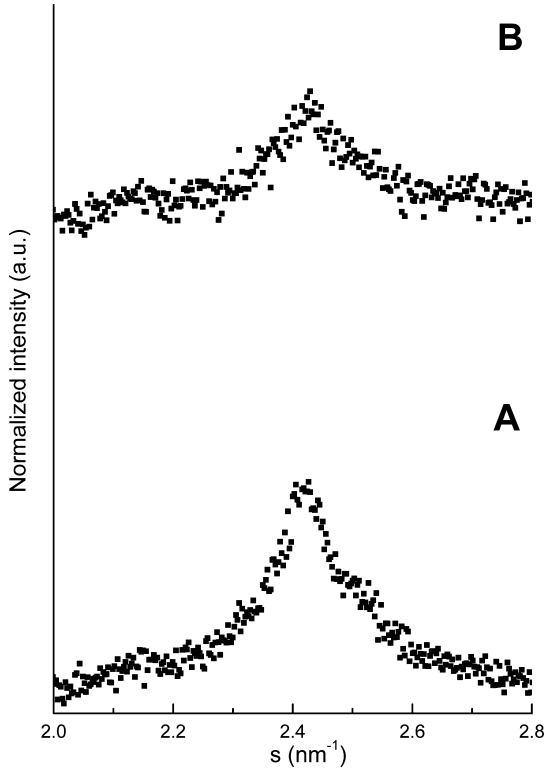

Figure 3. Wide-angle X-ray diffraction patterns of DMPC (A) and mixtures of DMPC with RFB at 10 mol % (B) at 10 °C.

on) exists. The zwitterionic species are more lipophilic in comparison to the charged ones.[3] Therefore, the zwitterionic species of RFB are expected to be inserted into the DMPC phospholipid bilayers according to their hydrophobicity gradient.[3] The hydrophilic imidazole and piperidine moieties should be inserted near the polar head groups of the phospholipids and hydrophobic naphthol should be embedded within the membranes, establishing van der Waals interactions with the hydrophobic tails.[13] This interaction is expected to cause a pronounced destabilization of the gel phases, which are characterized by a high degree of order and tight hydrocarbon chain packing in comparison with the fluid phase. Therefore, in the DMPC vesicles, the RFB location close to the head groups (C1−C9) is expected to produce an enhanced membrane perturbation.[14] In order to explore the influence of RFB on the T_m, SAXS and WAXS diffraction patterns of DMPC were taken on heating the sample. The results point to a marginal decrease of the DMPC main-transition temperature (T_m) even for high concentrations of RFB (data not shown).

3.2. Effects of RFB on the Structure of DMPG Bilayers.

Table 3 displays the long-range repeat distances (d) and the correlation length (ξ) between the DMPG bilayers in the absence and in the presence of RFB. The SAXS diffraction pattern (Figure 4A) of DMPG exhibits only a single broad peak, especially for higher temperatures. Thus, it was previously described that in charged phospholipids, due to the electrostatic repulsions, instead of the formation of MLVs, the formation of large unilamellar vesicles or of noncorrelated bilayers takes place. We did not analyze the broad peak in terms of a form factor of the DMPG bilayer. We only determined the d-spacings associated with a larger error bar (see Table 3).[11] The Bragg reflection peaks for DMPG appear at 1/47.9 Å^{-1} (Lβ'), 1/51.1 Å^{-1} (Pβ'), and 1/48.4 Å^{-1} (Lα), being in good agreement with literature data.[15]

Table 3. Long Distances (d) of DMPG Bilayers and Correlation Lengths (ξ) Determined from SAXS Diffraction Patterns at pH 7.4 and at 8, 18, and 40 °C[a]

sample (mol % RFB)	T (°C)	d_{SAXS} (Å)	ξ_1 (Å)
DMPG 0	8	47.9 ± 0.7	396 ± 10
	18	51.1 ± 0.7	421 ± 10
	40	48.4 ± 0.7	36 ± 10
DMPG:RFB 5	8	51.2 ± 0.7	324 ± 10
	18	48.1 ± 0.7	336 ± 10
	40	46.7 ± 0.7	23 ± 10
DMPG:RFB 10	8	51.5 ± 0.7	221 ± 10
	18	48.0 ± 0.7	171 ± 10
	40	45.9 ± 0.7	17 ± 10

[a]The data are presented in Å as a function of the 5 and 10 mol % RFB.

The WAXS patterns show an asymmetric Bragg peak centered around 1/4.03 and 1/3.86 Å^{-1}, typical of the pseudohexagonal lattice of the DMPG chains. Upon heating, one symmetric Bragg peak appears, centered around 1/4.04 Å^{-1}, indicating the formation of a hexagonal chain lattice with an unexpected small cross-sectional area of the chains (19 Å^2). Finally, at 40 °C, the characteristic broad band appears in the Lα phase (data not shown).[16] In addition, the expected melting transition at 22−24 °C was verified by SAXS and WAXS heating scans (data not shown). In fact, the ionic strength used (similar to the physiological conditions) is reported to preserve the narrow temperature interval of the phase transition from the gel to the liquid-crystalline phase similar to DMPC.[15] The analysis of the effect of RFB on the repeat distance of DMPG bilayers reveals that significant differences are observed for all

dx.doi.org/10.1021/jp403073v | J. Phys. Chem. B 2013, 117, 6187−6193

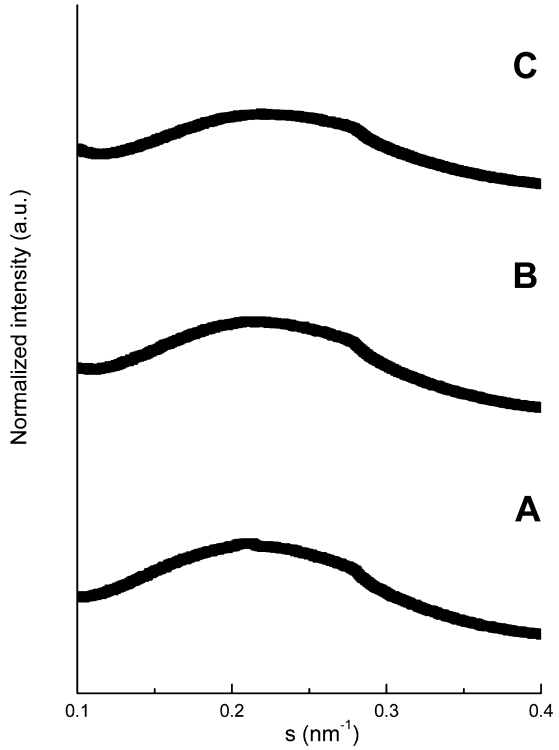

Figure 4. Small-angle X-ray diffraction patterns of DMPG (A) and mixtures of DMPG with RFB at 5 mol % (B) and 10 mol % (C) at 40 °C.

the phases of DMPG (Table 3). While the *d*-spacings increase in the Lβ' phase, they decrease both in the Pβ' and in the Lα phases with increasing RFB concentration. In addition, the correlation length (ξ) supports the observation that RFB disturbs the bilayer correlation in a concentration-dependent manner. On the other hand, the WAXS diffraction patterns (Table 4) indicate that RFB has a pronounced effect on the

Table 4. Short Distances (d) of DMPG Bilayers and Correlation Lengths (ξ) Determined from WAXS Diffraction Patterns at pH 7.4 and at 8, 18, and 40 °C[a]

		d_{WAXS} (Å)			
sample (mol % RFB)	T (°C)	d_1	d_2	ξ_1 (Å)	ξ_2 (Å)
DMPG 0	8	4.03	3.86	132 ± 10	14 ± 10
	18	4.04		177 ± 10	
DMPG:RFB 5	8	3.99		28 ± 10	
	18	3.98		24 ± 10	
DMPG:RFB 10	8	3.97		43 ± 10	
	18	3.97		31 ± 10	

[a]The data are presented in Å as a function of the 5 and 10 mol % RFB.

phospholipid chain packing. The single and symmetrical peak obtained in the presence of RFB is indicative of hexagonal hydrocarbon chain packing (data not shown). Surprisingly, the chain cross-sectional area decreases by incorporating RFB. This shows that RFB changes the effective area requirement of the phospholipid head groups, allowing a tighter packing of the chains.

On the other hand, the low correlation length (ξ) obtained (for both SAXS and WAXS measurements) may be attributed to the RFB ability to induce a marked disturbance in the DMPG bilayers. As mentioned above, at pH 7.4, RFB has a significant contribution of positively charged molecules that may establish electrostatic interactions with the deprotonated phosphate of DMPG. This effect could change the orientation of the phospholipid head groups and consequently allow the observed change in the chain packing. Moreover, the RFB interactions with the charged headgroup of DMPG might also be responsible for the observed decrease of the correlation length between the bilayers by a decrease of the stabilizing electrostatic repulsion.[11,16] The analysis of the heating scans shows that the T_m reported for DMPG, i.e., 22−24 °C, remains unchanged even for high drug concentrations (data not shown).

3.3. Effects of RFB on the Structure of DPPE:DPPG Bilayers. The SAXS diffraction patterns obtained for the DPPE:DPPG mixture in the gel phase at 37 °C in the absence and in the presence of RFB are presented in Figure 5. The

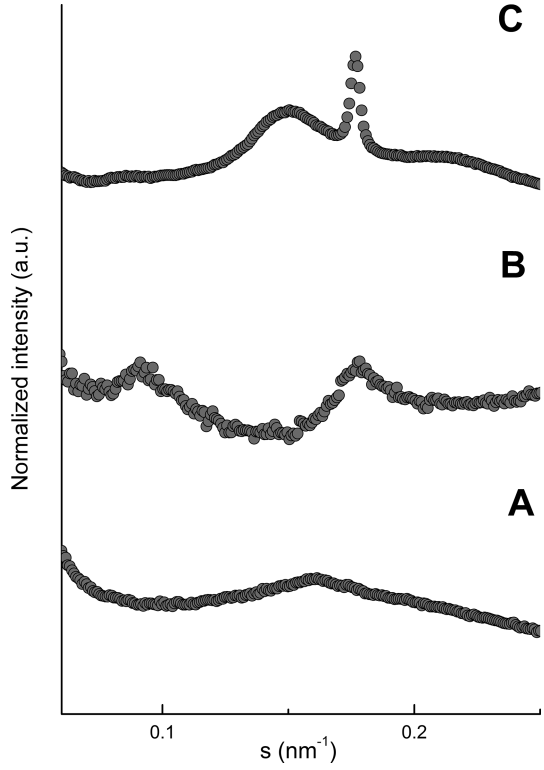

Figure 5. Small-angle X-ray diffraction patterns for DPPE:DPPG (A) and mixtures of DPPE:DPPG with RFB at 5 mol % (B) and 10 mol % (C) at 37 °C.

diffraction pattern with only one broad peak is clearly dominated by the 20% DPPG in this mixture. The broad peak observed in aqueous dispersions of anionic DPPG indicates the formation of noncorrelated bilayers in contrast to DPPE, which forms well-correlated bilayers characterized by a sharp Bragg peak.

The temperature of the main phase transition, determined using WAXS measurements, was 61−63 °C (data not shown) in accordance with the previously reported one for this lipid mixture.[17] Taking into account the phase transition temperatures of DPPE (63 °C) and DPPG (41 °C), the transition temperature is in contrast to the structure dominated by the 80% DPPE. DPPG and DPPE have the same chain pattern but completely different head groups. The headgroup of DPPG is negatively charged, while that of DPPE is zwitterionic but has a

dx.doi.org/10.1021/jp403073v | J. Phys. Chem. B 2013, 117, 6187−6193

Table 5. Long Distances (d) of DPPE:DPPG Bilayers and Correlation Lengths (ξ) Determined from SAXS Diffraction Patterns at pH 7.4 and at 37, 56, and 65 °C[a]

		d_{WAXS} (Å)			
sample (mol % RFB)	T (°C)	d_1	d_2	ξ_1 (Å)	ξ_2 (Å)
DPPE:DPPG 0	37	62.8 ± 0.5		137 ± 10	
	56	61.2 ± 0.5		317 ± 10	
	65	64.4 ± 0.5		202 ± 10	
DPPE:DPPG:RFB 5	37	117 ± 0.5		113 ± 10	
	56	110 ± 0.5		64 ± 10	
	65	114 ± 0.5		98 ± 10	
DPPE:DPPG:RFB 10	37	65.8 ± 0.5	56.6 ± 0.5	33 ± 10	1418 ± 10
	56	65.1 ± 0.5	56.1 ± 0.5	197 ± 10	1636 ± 10
	65	66.4 ± 0.5	56.1 ± 0.5	228 ± 10	1267 ± 10

[a]The data are presented in Å as a function of the 5 and 10 mol % RFB.

pronounced ability for hydrogen bond formation, being the main reason for the high T_m value.[8,18] In an ideal mixture, one would expect a transition temperature around 59 °C. The observed higher T_m indicates stronger interactions between the molecules in the mixture compared to the pure lipid systems. As shown in Figure 5, and as previously described, this lipid mixture exhibits only the broad scattering feature of MLVs or noncorrelated bilayers.[8,19] Nevertheless, we used the maximum of the broad peak to determine d-values: 1/62.8 Å^{-1} at 37 °C (gel phase), 1/61.2 Å^{-1} at 56 °C (gel phase), and 1/64.4 Å^{-1} at 65 °C (fluid phase), being concordant with literature data.[8] The WAXS pattern (Table 6) shows a single Bragg reflection at 1/4.07 Å^{-1} at 37 °C and 1/4.12 Å^{-1} at 56 °C, corresponding to the hexagonal chain packing in the gel phase. The cross-sectional area of the alkyl chains increases with increasing temperature in the gel phase from 19.1 to 19.6 Å^2. At 65 °C, the broad halo obtained is consistent with the chain melting (data not shown).[8]

The SAXS and to a moderate extent the WAXS patterns of DPPE:DPPG are influenced by the addition of RFB. The effect depends on the drug concentration. As shown in Figure 5 and Table 5, the addition of 5 mol % RFB is responsible for the appearance of two Bragg peaks in the s-ratio of 1:2 at all temperatures studied, characteristic of correlated bilayers. The interaction with RFB leads to a much better correlation between the bilayers but at a much larger distance of 110 Å. This larger d-value can only be explained by a much larger water layer between the bilayers. On the other side, 10 mol % RFB (Figure 5C) leads to a phase separation into DPPE-rich and DPPE-poor domains. The first ones are characterized by a sharp Bragg peak, as observed for pure DPPE, the second ones show the broad diffraction pattern typical for noncorrelated bilayers of DPPG. The WAXS diffraction pattern obtained for DPPG:DPPE in the presence of RFB (Table 6) exhibits also only one Bragg peak, independently of the drug concentration. Above 65 °C, the WAXS peak disappears, which is connected with the chain melting in the liquid crystalline phase (data not shown).[8] The correlation length (ξ) in the DPPE:DPPG bilayer (obtained by WAXS measurements) is not considerably influenced by RFB. In fact, RFB is an amphiphilic charged molecule with the ability to interact with charged phospholipid head groups. Therefore, it might be preferentially located at the hydrophilic/hydrophobic interface of a lipid bilayer stabilized by electrostatic interactions as well as hydrophobic interactions. Above a certain threshold concentration of RFB, the electrostatic interactions with DPPG lead to a phase separation in the lipid mixture.

Table 6. Short Distances (d) of DPPE:DPPG Bilayers and Correlation Lengths (ξ) Determined from WAXS Diffraction Patterns at pH 7.4 and at 37, 56, and 65 °C[a]

sample (mol % RFB)	T (°C)	d_{SAXS} (Å)	ξ_1 (Å)
DPPE:DPPG 0	**37**	4.07	132 ± 10
	56	4.12	177 ± 10
DPPE:DPPG:RFB 5	**37**	4.07	114 ± 10
	56	4.16	56 ± 10
DPPE:DPPG:RFB 10	**37**	4.07	175 ± 10
	56	4.17	176 ± 10

[a]The data are presented in Å as a function of the 5 and 10 mol % RFB.

4. CONCLUSIONS

In this work, the effect of RFB on human and bacterial membrane mimetic models (DMPC and DMPG, DPPE:DPPG) was evaluated using X-ray diffraction techniques. The overall results show that the interaction of the antimycobacterial drug RFB with the used membrane models is putatively related with the drug's mechanism of action. Therefore, the interaction of the drug with the membrane models is strongly dependent on the phospholipid head groups, the hydrocarbon chains, and the concentrations of the drug.

The effects of RFB on the DMPC bilayer are pronounced only in the gel phases. In the fluid Lα phase, the effects on the bilayer repeat distance are negligible. Therefore, the pronounced disordering effect of RFB on the gel phases of the DMPC bilayer might be related to some adverse effects caused by its ability to interact with some of the most ordered membranes of the human body, causing uveitis and the discoloration of the skin.[3] In fact, despite that most cell membranes exist in the fluid phase, the gel lamellar phase of lipid bilayers has biological relevance for specialized membranes such as stractum corneum.[20,21] Contrastingly to the effects of the antimycobacterial compound on the human membrane model (with a large amount of zwitterionic phosphatidylcholines), RFB has pronounced effects in the fluid phase (with most biological relevance) on the bacterial membrane model. In addition, RFB might exert a direct effect in the bacterial membrane. In fact, RFB (above a certain threshold) induces phase separation in the DPPG:DPPE mixture that can promote the membrane dysfunction due to increased permeability of the lipid bilayer.[8]

In summary, these results represent a contribution to the knowledge of the mechanism of action of RFB and might be

dx.doi.org/10.1021/jp403073v | J. Phys. Chem. B 2013, 117, 6187−6193

useful for the development of more potent antibiotics with fewer side effects.

AUTHOR INFORMATION

Corresponding Author

*Address: REQUIMTE, Departamento de Ciências Químicas, Faculdade de Farmácia, Universidade do Porto Rua de Jorge Viterbo Ferreira n.° 228 4050-313 Porto, Portugal. E-mail: shreis@ff.up.pt. Phone: +351-220428672. Fax: +351-226093483.

Notes

The authors declare no competing financial interest.

ACKNOWLEDGMENTS

M.P., J.M.C., and C.N. thank FCT (Lisbon) for the fellowships (SFRH/BD/63318/2009, SFRH/BD/66789/2009, and SFRH/BPD/81963/2011, respectively). The authors are also grateful to the FCT for financial support under projects PEst-OE/QUI/UI0612/2011 and PTDC/QUI-QUI/101022/2008 with coparticipation European Community funds from the FEDER, QREN, and COMPET. The authors thank HASYLAB at DESY, Hamburg, Germany, for beam time and support through the project II-20100139 EC. The authors are grateful to Dr. Sérgio Funari for help at beamline A2.

REFERENCES

(1) Aristoff, P. A.; Garcia, G. A.; Kirchhoff, P. D.; Hollis Showalter, H. D. Rifamycins–Obstacles and Opportunities. *Tuberculosis* **2010**, *90* (2), 94−118.

(2) Figueiredo, R.; Moiteiro, C.; Medeiros, M. A.; da Silva, P. A.; Ramos, D.; Spies, F.; Ribeiro, M. O.; Lourenco, M. C.; Junior, I. N.; Gaspar, M. M.; Cruz, M. E.; Curto, M. J.; Franzblau, S. G.; Orozco, H.; Aguilar, D.; Hernandez-Pando, R.; Costa, M. C. Synthesis and Evaluation of Rifabutin Analogs against Mycobacterium avium and H(37)Rv, MDR and NRP Mycobacterium tuberculosis. *Bioorg. Med. Chem.* **2009**, *17* (2), 503−511.

(3) Pinheiro, M.; Arede, M.; Nunes, C.; Caio, J. M.; Moiteiro, C.; Lucio, M.; Reis, S. Differential Interactions of Rifabutin with Human and Bacterial Membranes: Implication for Its Therapeutic and Toxic Effects. *J. Med. Chem.* **2013**, *56* (2), 417−426.

(4) Pereira-Leite, C.; Carneiro, C.; Soares, J. X.; Afonso, C.; Nunes, C.; Lucio, M.; Reis, S. Biophysical Characterization of the Drugs-Membrane Interaction: The Case of Propranolol and Acebutolol. *Eur. J. Pharm. Biopharm.* **2013**, *84*, 183−191.

(5) Maloney, E.; Stankowska, D.; Zhang, J.; Fol, M.; Cheng, Q. J.; Lun, S.; Bishai, W. R.; Rajagopalan, M.; Chatterjee, D.; Madiraju, M. V. The Two-Domain LysX Protein of Mycobacterium tuberculosis Is Required for Production of Lysinylated Phosphatidylglycerol and Resistance to Cationic Antimicrobial Peptides. *PLoS Pathog.* **2009**, *5* (7), e1000534.

(6) Rappolt, M.; Hickel, A.; Bringezu, F.; Lohner, K. Mechanism of the Lamellar/Inverse Hexagonal Phase Transition Examined by High Resolution X-ray Diffraction. *Biophys. J.* **2003**, *84* (5), 3111−3122.

(7) Pili, B.; Bourgaux, C.; Meneau, F.; Couvreur, P.; Ollivon, M. Interaction of an Anticancer Drug, Gemcitabine, with Phospholipid Bilayers. *J. Therm. Anal. Calorim.* **2009**, *98* (1), 19−28.

(8) Oszlanczi, A.; Bota, A.; Klumpp, E. Influence of Aminoglycoside Antibiotics on the Thermal Behaviour and Structural Features of DPPE-DPPG Model Membranes. *Colloids Surf., B* **2010**, *75* (1), 141−148.

(9) Eisenblatter, J.; Winter, R. Pressure Effects on the Structure and Phase Behavior of DMPC-Gramicidin Lipid Bilayers: a Synchrotron SAXS and 2H-NMR Spectroscopy Study. *Biophys. J.* **2006**, *90* (3), 956−966.

(10) Nunes, C.; Brezesinski, G.; Lima, J. L.; Reis, S.; Lucio, M. Synchrotron SAXS and WAXS Study of the Interactions of NSAIDs with Lipid Membranes. *J. Phys. Chem. B* **2011**, *115* (24), 8024−8032.

(11) Cardoso, A. M.; Trabulo, S.; Cardoso, A. L.; Lorents, A.; Morais, C. M.; Gomes, P.; Nunes, C.; Lucio, M.; Reis, S.; Padari, K.; Pooga, M.; Pedroso de Lima, M. C.; Jurado, A. S. S4(13)-PV Cell-Penetrating Peptide Induces Physical and Morphological Changes in Membrane-Mimetic Lipid Systems and Cell Membranes: Implications for Cell Internalization. *Biochim. Biophys. Acta* **2012**, *1818* (3), 877−888.

(12) Grabielle-Madelmont, C.; Hochapfel, A.; Ollivon, M. Antibiotic−Phospholipid Interactions as Studied by DSC and X-ray Diffraction. *J. Phys. Chem. B* **1999**, *103* (21), 4534−4548.

(13) Vostrikov, V. V.; Selishcheva, A. A.; Sorokoumova, G. M.; Shakina, Y. N.; Shvets, V. I.; Savel'ev, O. Y.; Polshakov, V. I. Distribution Coefficient of Rifabutin in Liposome/Water System as Measured by Different Methods. *Eur. J. Pharm. Biopharm.* **2008**, *68* (2), 400−405.

(14) Nunes, C.; Brezesinski, G.; Pereira-Leite, C.; Lima, J. L. F. C.; Reis, S.; Lúcio, M. NSAIDs Interactions with Membranes: A Biophysical Approach. *Langmuir* **2011**, *27* (17), 10847−10858.

(15) Duarte, E. L.; Oliveira, T. R.; Alves, D. S.; Micol, V.; Lamy, M. T. On the Interaction of the Anthraquinone Barbaloin with Negatively Charged DMPG Bilayers. *Langmuir* **2008**, *24* (8), 4041−4049.

(16) Spinozzi, F.; Paccamiccio, L.; Mariani, P.; Amaral, L. Q. Melting Regime of the Anionic Phospholipid DMPG: New Lamellar Phase and Porous Bilayer Model. *Langmuir* **2010**, *26* (9), 6484−6493.

(17) Sevcsik, E.; Pabst, G.; Richter, W.; Danner, S.; Amenitsch, H.; Lohner, K. Interaction of LL-37 with Model Membrane Systems of Different Complexity: Influence of the Lipid Matrix. *Biophys. J.* **2008**, *94* (12), 4688−4699.

(18) Chen, X.; Huang, Z.; Hua, W.; Castada, H.; Allen, H. C. Reorganization and Caging of DPPC, DPPE, DPPG, and DPPS Monolayers Caused by Dimethylsulfoxide Observed Using Brewster Angle Microscopy. *Langmuir* **2010**, *26* (24), 18902−18908.

(19) Urbán, E.; Bóta, A.; Kocsis, B. Non-Bilayer Formation in the DPPE−DPPG Vesicle System Induced by Deep Rough Mutant of Salmonella minnesota R595 Lipopolysaccharide. *Colloids Surf., B* **2006**, *48* (2), 106−111.

(20) Norlen, L. Skin Barrier Structure and Function: the Single Gel Phase Model. *J. Invest. Dermatol.* **2001**, *117* (4), 830−836.

(21) Tristram-Nagle, S.; Liu, Y.; Legleiter, J.; Nagle, J. F. Structure of Gel Phase DMPC Determined by X-ray Diffraction. *Biophys. J.* **2002**, *83* (6), 3324−3335.